Journal of Inorganic Biochemistry 115 (2012) 36–43

Contents lists available at SciVerse ScienceDirect

Journal of Inorganic Biochemistry

journal homepage: www.elsevier.com/locate/jinorgbio

Synthesis, crystal structure, characterisation, and antifungal activity of 3-thiophene aldehyde semicarbazone (3STCH), 2,3-thiophene dicarboxaldehyde bis(semicarbazone) (2,3BSTCH$_2$) and their nickel (II) complexes

Kusaï Alomar [a], Vincent Gaumet [b], Magali Allain [c], Gilles Bouet [a,*], Anne Landreau [a]

[a] Laboratoire SONAS, EA 921, Université d'Angers, IFR QUASAV 149, UFR Sciences Pharmaceutiques et Ingénierie de la Santé, 16 Boulevard Daviers, F-49045 Angers cedex 01, France
[b] UMR 990 Inserm, Imagerie Moléculaire et Thérapie Vectorisée, Université d'Auvergne, Faculté de Pharmacie, 28 place Henri Dunant, 63001 Clermont-Ferrand cedex 1, France
[c] Institut des Sciences et Technologies Moléculaires d'Angers (MOLTECH-Anjou), UMR CNRS 6200, Université d'Angers, 2 Boulevard Lavoisier, 49045 Angers cedex 01, France

ARTICLE INFO

Article history:
Received 1 February 2012
Received in revised form 23 April 2012
Accepted 24 April 2012
Available online 24 May 2012

Keywords:
Thiophene
Semicarbazone
Crystal structure
Nickel complexes
Antifungal activity
Cytotoxicity

ABSTRACT

The reaction of nickel (II) chloride and bromide with 3-thiophene aldehyde semicarbazone (3STCH) and 2,3-thiophene dicarboxaldehyde bis(semicarbazone) (2,3BSTCH$_2$) leads to the formation of a series of new complexes: [NiCl$_2$(3STCH)$_2$], [NiBr$_2$(3STCH)$_2$], [NiCl(2,3BSTCH$_2$)(H$_2$O)]Cl, and [NiBr(2,3BSTCH$_2$)(H$_2$O)]Br respectively. The crystal structures of the two ligands 3STCH, 2,3BSTCH$_2$ and of the complex [NiBr(2,3BSTCH$_2$)(H$_2$O)]Br have been determined by X-ray diffraction methods. For all these complexes, the central ion is coordinated through the oxygen atom of the carbonyle and the azomethine nitrogen atom of the semicarbazone. The antifungal activity of the complexes and their corresponding ligands was evaluated against some strains of respectively, *Candida albicans*, *Candida glabrata* and *Aspergillus fumigatus*. The complexes with 3STCH and 2,3BSTCH$_2$ revealed interesting CMI$_{80}$ values specifically against *C. glabrata*. Cytotoxicity assay was also carried out in vitro on MRC5 cells.

1. Introduction

Thiosemicarbazones, semicarbazones and their metal complexes have been extensively studied in recent years [1,2], mainly because of their various biological and antimicrobial properties [3–5]. Semicarbazones usually act as chelating ligands with transition metal ions, bonding through the carbonyle oxygen and the hydrazine nitrogen atoms [6].

However, semicarbazonescharacha have received much less attention than their sulphur-containing analogues. As a contribution to a better understanding of this versatile class of compounds [7], the heterocyclic semicarbazones (e.g.: furans) which functional group attached at 2-position, have been the subjects of extensive investigation for their structural studies as well as their potent biological properties [7,8]. Chemically speaking, the heterocyclic semicarbazones are of high interest because of their versatility as ligands. This is due to the presence of several potential donor atoms, their flexibility, and their ability to coordinate either in neutral or deprotonated forms because of their tautomerism equilibrium leading to keto and enol forms [9]. So they are compounds with versatile structural features and they can coordinate to the metal either as a neutral ligand or as a deprotonated anion.

We have previously described the furanic semicarbazones: 2-furaldehyde semicarbazone, 5-methyl 2-furfural semicarbazone and 3-(2-furyl)prop-2-enal semicarbazone [10,11]. In this series, the nickel (II) complexes showed an octahedral geometry, coordinating through the oxygen atom of the furan ring and the imino nitrogen atom. Many examples of pharmacological applications with this class of compounds have been evaluated for their antitumor [12], antibacterial [13,14] and antifungal [15,16] activities. In many cases, upon coordination to metal ions, the bioactivity of these organic compounds increases [17,18] and sometimes with a decreased toxicity [19]. As a part of our continuous research work pertaining to the synthesis, the characterisation and the biological activity of metal complexes from semicarbazones and thiosemicarbazones with five-membered heterocycles [19,20], we describe here some new transition metal complexes obtained from 3-thiophenaldehyde semicarbazone (3STCH) and 2,3-thiophene dialdehyde bis(semicarbazone) (2,3BSTCH$_2$) (Fig. 1) as ligands and nickel (II) chlorides and bromides. In addition, the crystal structures of the ligands and of the complex [NiBr(2,3BSTCH$_2$)(H$_2$O)]Br are described. The antifungal activities of the two ligands and their complexes were evaluated against *Candida albicans*, *Candida glabrata* and *Aspergillus fumigatus*. Moreover, the evaluation in vitro of their cytotoxicity towards MRC5 cells was performed.

2. Experimental

2.1. Reactants

All reactants and solvents were of analytical grade. Semicarbazide hydrochloride and thiophene-3-carboxaldehyde were purchased from

* Corresponding author. Tel.: +33 2 41 22 66 00; fax: +33 2 41 22 66 34.
E-mail address: gilles.bouet@univ-angers.fr (G. Bouet).

0162-0134/$ – see front matter © 2012 Elsevier Inc. All rights reserved.
doi:10.1016/j.jinorgbio.2012.04.022

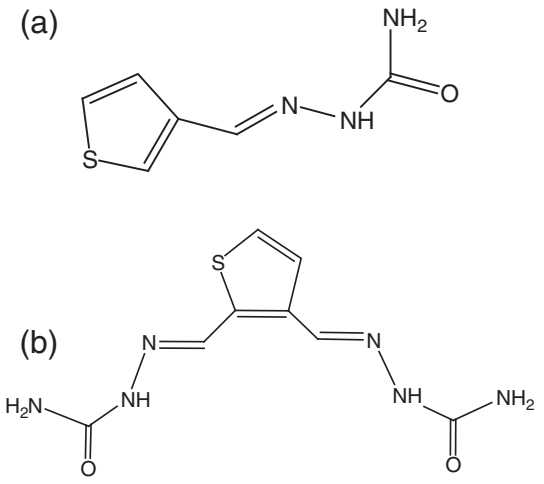

Fig. 1. Chemical structure of the ligands: (a) 3-thiophene carboxaldehyde semicarbazone (3STCH), (b) 2,3-thiophene dicarboxaldehyde bis(semicarbazone) ($2,3BSTCH_2$).

Alfa Aesar, thiophene-2,3-dicarboxaldehyde from Aldrich (France). Nickel hydrated salts (Prolabo) were used as received.

2.2. Measurements

Elemental analyses were carried out by the service central of analyses (C.N.R.S. Vernaison, France) or by Plateforme Intégrée d'Analyse Moléculaire (PIAM), Faculté des Sciences, Université d'Angers (France). DSC diagrams were recorded in the 25–400 °C range with a Mettler DSC 822e unit, with the help of Mettler Toledo STAR^e SW 8.10 System software (Laboratoire de Physique, Faculté de Pharmacie, Angers); the heating rate was 10 °C per min. All measurements were made in 40 mm^3 closed Al crucibles. The IR spectra were recorded with a Bruker FTIR Vector 22 spectrometer between 4400 and 400 cm^{-1} (KBr discs). The far IR spectra were recorded with a Bruker Vertex FTIR spectrophotometer in the 650 to 50 cm^{-1} range using polyethylene discs (Institut des Matériaux Jean Rouxel, université de Nantes (France)).

2.3. Crystal data collection and processing

Crystals of the ligands 3STCH, and $2,3BSTCH_2$ are monoclinic with space group $P2_1/c$. The crystal and instrumental parameters used in the unit-cell determination and data collection are summarised in Table 1. X-ray single-crystal diffraction data were collected at 293 K on a STOE-IPDS diffractometer for 3STCH and on a BRUKER-NONIUS KappaCCD diffractometer for $2,3BSTCH_2$, both equipped with a graphite monochromator using MoK_α radiation ($\lambda = 0.71073$ Å) (MOLTECH-Anjou, UMR CNRS 6200, Université d'Angers). The structures were solved by direct methods and refined on F^2 by full-matrix least-squares method with anisotropic approximation for all non-hydrogen atoms, using SHELX97 package [21]. For 3STCH, absorption was corrected by Gaussian technique and the H atoms were found by Fourier difference synthesis. For $2,3BSTCH_2$, absorption was corrected by SADABS programme (Sheldrick, Bruker, 2000) and the H atoms were included in the calculation without refinement.

The complex [NiBr($2,3BSTCH_2$)(H_2O)]Br was crystallised from a water–ethanol mixture at room temperature as pale yellow plates. A crystal $0.07 \times 0.23 \times 0.51$ mm^3 in size was placed and optically centred on a Bruker KAPPA APEX II diffractometer equipped with a Mo Kα radiation ($\lambda = 0.71073$ Å) at 293 (2) K. The initial unit cell was indexed using the difference vectors method of a random set of reflections collected from three series of 0.5° wide omega-scans, 20 s per frame, and 12 frames per series that were well distributed in reciprocal space. The crystal to detector distance was 50 mm. A total of 1064 frames were collected to $\theta_{max} = 28.8°$ with 0.5° wide scans and an exposure time of 10 s per frame using the APEX2 software [22]. Unit cell refinement on all observed reflections and data reduction were performed using SAINT [23]. Scaling and a numerical absorption correction, based upon crystal size and faces indexing, were done using SADABS [23]. The minimum and maximum transmission factors were 0.167 and 0.621, respectively. Systematic absences and intensity statistics were consistent with the compound having crystallised in the centrosymmetric monoclinic space group $P2_1/c$. A total of 12,282 reflections were collected, merged based upon identical indices yielding 3877 data ($R_{int} = 0.031$) which 3123 had $I > 2\sigma(I)$.

Table 1
Crystallographic data.

Name	3STCH	$2,3BSTCH_2$	[NiBr($2,3BSTCH_2$)(H_2O)]Br
Formula	$C_6H_7N_3OS$	$C_8H_{10}N_6O_2S$	$C_8H_{12}NiBr_2N_6O_3S$
Formula weight	169.21	254.28	490.80
Crystal system	Monoclinic	Monoclinic	Monoclinic
Space group	$P2_1/c$	$P2_1/c$	$P2_1/c$
a (Å)	11.523 (2)	10.2925 (9)	6.8882 (4)
b (Å)	5.4289 (5)	15.5806 (6)	7.2754 (4)
c (Å)	12.524 (2)	13.908 (1)	29.9878 (19)
α (°)	90	90	90
β (°)	102.09 (2)	97.615 (9)	95.491 (3)
γ (°)	90	90	90
V (Å^3)	766.1 (2)	2210.7 (3)	1495.93 (15)
Z	4	8	4
Colour	Yellow	Yellow	Green dark
D_{calc} ($g.cm^{-3}$)	1.454	1.528	2.179
Crystal size (mm)	$0.54 \times 0.23 \times 0.08$	$0.3 \times 0.13 \times 0.08$	$0.51 \times 0.23 \times 0.07$
μ (mm^{-1})	0.364	0.294	6.796
hkl limits	$-14 \le h \le 14$ $-6 \le k \le 6$ $-15 \le l \le 15$	$-13 \le h \le 13$ $-20 \le k \le 20$ $-18 \le l \le 18$	$-9 \le h \le 9$ $-9 \le k \le 9$ $-40 \le l \le 37$
θ_{min}, θ_{max} (°)	1.81, 26.07	2.94, 27.51	2.7, 28.8
R1 for $I > 2\sigma(I)$	0.0466	0.0699	0.035
wR_2 for $I > 2\sigma(I)$	0.1099	0.1144	0.11

The structure was determined by direct methods with the successful location of all non-hydrogen atoms of the unique molecule within the asymmetric unit using the programme SHELXS [24]. The structure was refined with SHELXL [21]. All non-hydrogen atoms were refined anisotropically. Rotation of the thienyl ring by 180° causes the sulphur atom and the C(2)–H group to change places, the C(3) converting to C(4) and vice versa. Bearing in mind that the van der Waals volume of C–H group is close to the volume of a sulphur atom both conformations can be realised in the same crystallographic position [25]. This leads to a static disordering in the crystal structure. The values of the free factors which identify the population densities of the atoms are 0.840(6) for the first thienyl description (atoms A) and 0.160(6) for the second thienyl description (atoms B). Best results have been obtained when couples C1A/C1B, C3A/C4B, and C4A/C3B are constrained to same positions. The hydrogen atoms were included in calculated positions according to their geometry and refined riding on carbon atoms. Hydrogen atoms linked to oxygen of water molecule were located in subsequent difference Fourier maps, refined and geometrically restrained to the same distance (DFIX command of SHELXL97). The final structure was refined to convergence with R(F) = 3.52% and GOOF = 1.091 for those 3123 data with $Fo > 4\sigma(Fo)$ [R(F) = 5.05% and GOOF = 1.108 for all 3877 data]. An empirical correction for extinction was also attempted but found to be equal to zero within the error and therefore not applied.

2.4. Biological activities

2.4.1. Microorganisms

Antifungal activity was assayed on human pathogenic fungi, including yeasts of the *Candida* genus: *C. albicans* (ATCC 66396), *C. glabrata* (LMA 90-1085), and one opportunistic mould *A. fumigatus* (CBS 11326). All

fungi were obtained from the parasitology and mycology laboratory of the CHU of Angers. Moulds were cultivated at 37 °C on yeast extract–peptone–dextrose agar (YPDA) containing 0.5 $g.L^{-1}$ chloramphenicol for 2 days for yeasts and 3 days for *A. fumigatus*.

2.4.2. Determination of antifungal activity

Tests were performed by following the guidelines of the approved reference method for yeasts (NCCLS document M27A) [26] and according to the NCCLS guidelines for filamentous fungi (M38-P) [27]. Briefly, the yeast suspensions were prepared in RPMI-1640 culture medium and adjusted spectrophotometrically at 630 nm to reach a final concentration of ca. 0.5×10^3 to 2.5×10^3 cells per mL. The tests were performed using sterile 96 flat shaped well microtitre plates. Serial two-fold drug dilutions were made in DMSO. Drugs were dispensed at a volume of 5 μL in triplicate into the wells to obtain final concentrations from 250 to 1.95 $\mu g.mL^{-1}$. After 48 h at 37 °C for the yeasts, and 72 h for *A. fumigatus*, the spectrophotometric MIC endpoint was calculated from the turbidimetric data as the lowest drug concentration giving rise to an inhibition of growth equal to or greater than 80% of that the drug-free control (MIC_{80}). Amphotericine B was used as a positive control.

DMSO activity was evaluated from 10 to 0.075% final concentrations, according in the same way. The tests were performed using sterile 96 flat shaped well microtitre plates. For each dilution, 20 μL of DMSO was added to 180 μL of RPMI medium previously inoculated with yeasts or *A. fumigatus*. After an incubation of 48 h at 37 °C for the yeasts and 72 h for *A. fumigatus*, the spectrophotometric MIC endpoint were calculated from the turbidimetric data compared to that of the DMSO-free control. The chosen threshold was 2.5% final concentration in DMSO because growth was still significant with respectively 71% for *A. fumigatus* and 86% for yeasts.

2.4.3. Cytotoxicity

Cytotoxicity was evaluated at Institut de Chimie des Substances Naturelles, CNRS UPR 2301 (Gif sur Yvette, France) on MRC5 cells in DMSO at 10^{-5} and 10^{-6} M according to the procedure described by Moret et al. [28]. Taxotere was used as the reference substance.

2.5. Synthesis of the ligands

2.5.1. Synthesis of 3STCH

This ligand was obtained from thiophene-3-carboxaldehyde and semicarbazide hydrochloride (1:1 M ratio). To a solution (MeOH) of semicarbazide hydrochloride (1 g; 9 mmol; 15 mL), potassium hydroxide (0.5 g; 15 mL; MeOH) was added, after 10 min KCl precipitated. The solution was filtered and a solution of thiophene-3-carboxaldehyde (1 g; 9 mmol; 15 mL; EtOH) was added. The mixture was refluxed for 1 h and then cooled. The ligand was removed by filtration and recrystallised from ethanol. Yellow single crystals suitable for X-ray analysis were grown [29].

2.5.2. Synthesis of 2,3BSTCH$_2$

This ligand was prepared from thiophene-2,3-dicarboxaldehyde and semicarbazide (1:2 M ratio) obtained as described above. The mixture was refluxed for 3 h and then cooled. The solid was filtered and recrystallised from ethanol [30]. Yellow single crystals suitable for X-ray analysis were grown at room temperature by slow evaporation of a mixture of ethanol (50%) and water (50%).

2.6. Preparation of the complexes

All the complexes with 3STCH were prepared starting from 5 mmol (0.85 g) of 3STCH dissolved in EtOH. The ethanolic solution of the metal halide was added slowly while stirring. The complexes were removed by filtration, washed with MeOH and finally dried in vacuum over silica gel. All the complexes with 2,3BSTCH$_2$ were prepared from 2.5 mmol (0.64 g) of 2,3BSTCH$_2$ according to the individual procedure described below.

2.6.1. Dichloro bis(3-thiophenaldehyde semicarbazone) nickel (II) [$NiCl_2$(3STCH)$_2$]

$NiCl_2\cdot6H_2O$ (0.64 g; 2.5 mmol; 10 mL) was added to the 3STCH ethanolic solution (20 mL) was maintained at room temperature for 4 h [3].

2.6.2. Dibromo bis(3-thiophenaldehyde semicarbazone) nickel (II) [$NiBr_2$(3STCH)$_2$]

$NiBr_2\cdot x\,H_2O$ (0.59 g; 2.5 mmol; 10 mL) was added to the ethanolic solution of 3STCH (20 mL) under refluxing conditions. The reflux was maintained for 6 h.

2.6.3. {Aqua chloro [2,3-thiophenaldehyde bis(semicarbazone)] nickel (II)} chloride [NiCl(2,3BSTCH$_2$)(H_2O)]Cl

$NiCl_2\cdot6\,H_2O$ (0.64 g; 2.5 mmol; H_2O; 10 mL) was added to 2,3BSTCH$_2$ (0.64 g; 2.5 mmol; EtOH; 10 mL) in a sealed flask and heated up to reflux under pressure for 24 h. After cooling, the solution is concentrated under reduced pressure until the complex precipitated.

2.6.4. {Aqua bromo [2,3-thiophenaldehyde bis(semicarbazone)] nickel (II)} bromide [NiBr(2,3BSTCH$_2$)(H_2O)]Br

This complex was obtained in the same way than the corresponding chloro compound, starting from $NiBr_2$ (0.59 g; 2.5 mmol; H_2O; 10 mL) and 2,3BSTCH$_2$ (0.64 g; 2.5 mmol; EtOH; 10 mL).

3. Results and discussion

3.1. Crystal structure of 3STCH

The main crystal parameters are reported in Table 1. The monoclinic unit cell (space group $P2_1/c$) contains four molecules. The molecule of 3STCH with numbering scheme is given in Fig. 2. The molecule 3STCH is quite planar with a feeble mean deviation to the plane. The most important deviation is observed for C3: 0.063 Å. The oxygen atom O1 and the hydrazone nitrogen N3 are in *E* position with respect to the C1 – N2 bond. This configuration is often observed in semicarbazones and its stability is due to the presence of an intramolecular hydrogen bond between N3-imino atom and H1B from NH_2, this interaction is weak but sufficient to stabilise the *E* configuration.

Representative bond distances and angles for 3STCH are shown in Table 2. The C1 – O1 bond length (1.239 Å) is typical of a double bond. The length of the C2 – N3 bond is 1.275 Å while the length of N2 – N3 is 1.375 Å. These distances are typical of a C═N double bond and an N – N single bond respectively [6].

The packing arrangement in the unit cell is given in Fig. 3a. The packing of a group of independent molecules is governed by N – H… O hydrogen bonds (Table 4, Fig. 3b). They are consistent with those

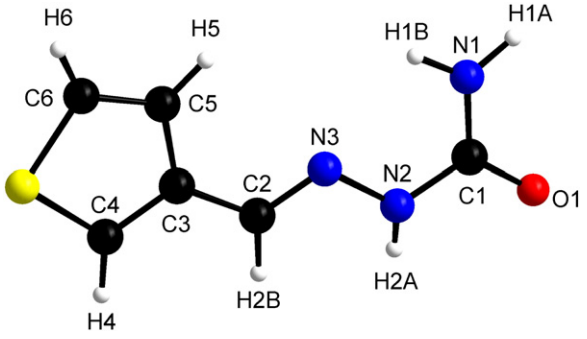

Fig. 2. Crystal structure and atoms numbering for 3STCH.

observed in the case of the *P*-dimethylaminobenzaldehyde semicarbazone where similar intermolecular N–H…O hydrogen bonds occurred [31].

3.1.1. Crystal structure of 2,3BSTCH$_2$

The main crystal parameters are reported in Table 1. Some representative bond lengths and angles are reported in Table 3. The monoclinic unit cell (space group $P2_1/c$) contains eight molecules in four groups of tow independent molecules. The tow independent molecules with numbering scheme are given in Fig. 4. The first and the second molecules lie in quite parallel planes with a 9.595° deviation.

Each of the tow independent molecules is quite planar with a feeble mean deviation to the plane. The most important deviations observed are as follows: N6: 0.195 Å, N8: 0.247 Å, N9: 0.478 Å, N11: 0.212 Å, N12: 0.341 Å and C9: 0.392 Å. The oxygen atom O1 and the hydrazone nitrogen N1 are in *E* position with respect to the C6–N2 bond, the same configuration is observed for O2 and N4 referring to C8–N5 bond. Its stability is due to the presence of an intramolecular hydrogen bond between N-imino atom and H from NH_2. The distances N1–H3B, N4–H6B, N7–H9B, N10–H12B are 2.326, 2.299, 2.296 and 2.288 Å respectively and consequently these interactions are weak, but sufficient to stabilise the *E* configuration [32].

Some very slight differences appear in the bond distances and angles in the semicarbazone moiety between the two molecules. Representative bond distances and angles for the two independent molecules are shown in Table 3. The C–O bond lengths (1.240, 1.246 Å) are typical of a C═O double bond. The bond lengths of the C5–N1 and C7–N4 bonds are 1.271 and 1.283 Å respectively, these distances are typical of a C═N. That the bond length of N1–N2, N4–N5 is 1.378, 1.369 Å respectively, these distances correspond to an N–N single bond and similar values are observed for the second independent molecule. Similar values were observed in the cases of diaqua[2,6-diacetylpyridine bis(semicarbazone)]chromium (III) hydroxide dinitrate hydrate and dichloro[2,6-diacetylpyridine bis(semicarbazone)]iron (III) chloride dihydrate complexes [33] and manganese (II) complex with 2,6-diacetylpyridine bis(2-aminobenzoylhydrazone) as well [34].

The packing arrangement in the unit cell is given in Fig. 5 and it is governed by intermolecular hydrogen bonds. The molecules are stacked in parallel planes along *b* axis and the intermolecular hydrogen bonding (Table 5) occurred through carbonyl oxygen atoms. The first independent molecule gives 5 hydrogen bonds: O1 with H11 and H9B; O2 linked with H2A, H9A and H12A. Four hydrogen bonds are observed in the second independent molecule: O3 with H5A and H3B and O4 with H3A and H6A. All these intermolecular hydrogen bonds are located between neighbour sets of two independent molecules and, inside a set, there is no hydrogen bond between the two molecules.

3.2. Crystal structure of the nickel complex [NiBr(2,3BSTCH$_2$)(H$_2$O)]Br

Relevant crystal data for [NiBr(2,3BSTCH$_2$)(H$_2$O)]Br is given in Table 1. A perspective view of [NiBr(2,3BSTCH$_2$)(H$_2$O)]Br compound with the atom numbering scheme is shown in Fig. 6.

The complex molecule is quite planar and its *E*, *E*′ configuration allows Ni^{2+} to adopt a (4 + 2) surrounding. The equatorial positions are occupied by two nitrogen and the two oxygen atoms of the 2,3BSTCH$_2$ molecule, acting as a tetradentate ligand, and the apical positions are occupied by a bromide ion and the oxygen atom of the water molecule. The four basal atoms are coplanar with O2–Ni1–N1 and N4–Ni1–O1 angles of 173.58° and 176.14° respectively. The corresponding bond pairs have nearly the same length. The basal bond distances Ni1–N1, Ni1–N4, Ni1–O1 and Ni1–O2 are 2.013 Å, 2.018 Å, 2.021 Å and 2.011 Å respectively (Table 4). The elongated axial bond length Ni1–O3 (water) is 2.143 Å and angle between O3–Ni1–Br1 is 178.38° [35].

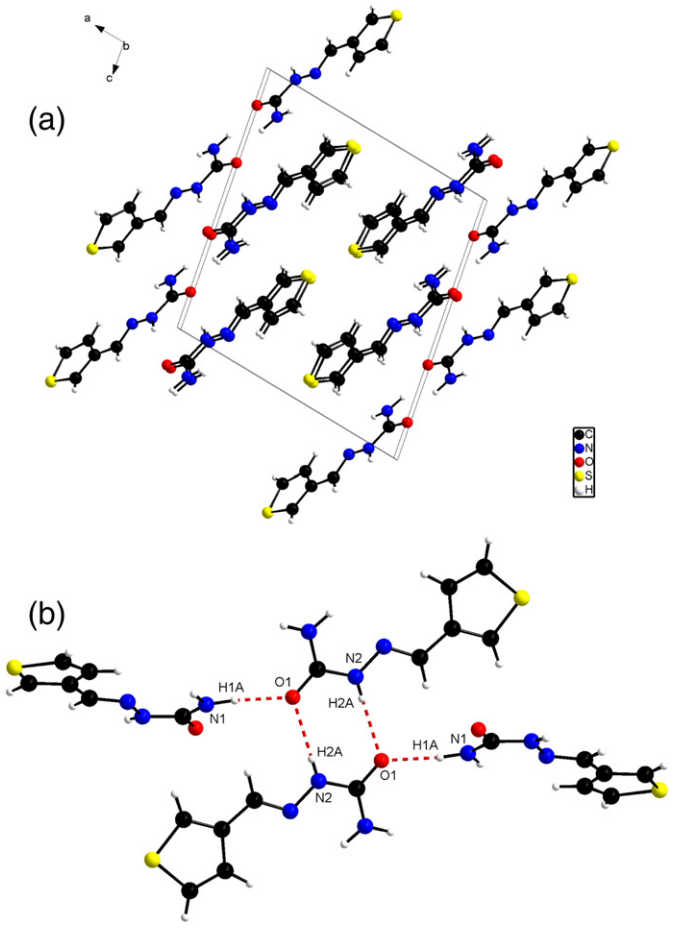

Fig. 3. Cell packing (a) and hydrogen bonding (b) for 3STCH.

Table 2
Selected bond lengths (Å) and angles (°) of 3STCH.

Bond lengths		Bond angles	
C1–N1	1.330	N1–C1–N2	116.74
C1–N2	1.363	N1–C1–O1	124.35
C1–O1	1.239	N2–C1–O1	118.90
C2–N3	1.275	C1–N2–N3	119.76
N2–N3	1.375	C2–N3–N2	115.35

Table 3
Selected bond lengths (Å) and angles (°) of 2,3BSTCH$_2$.

Bond lengths		Bond angles	
C5–N1	1.271	N1–C5–C3	124.5 (3)
C6–O1	1.240	O1–C6–N3	124.0 (3)
C6–N3	1.332	O1–C6–N2	118.9 (3)
C6–N2	1.353	N3–C6–N2	117.1 (3)
C7–N4	1.283	N4–C7–C4	120.0 (3)
C8–O2	1.246	O2–C8–N6	123.4 (3)
C8–N6	1.341	O2–C8–N5	119.4 (3)
C8–N5	1.357	N6–C8–N5	117.1 (3)
C13–N7	1.277	N7–C13–C11	123.4 (3)
C14–O3	1.236	O3–C14–N9	124.0 (3)
C14–N9	1.333	O3–C14–N8	119.4 (3)
C14–N8	1.368	O4–C16–N12	122.8 (3)
C15–N10	1.286	O4–C16–N11	120.2 (3)
C16–O4	1.233	N9–C14–N8	116.6 (3)
C16–N12	1.330	N12–C16–N11	117.0 (3)
C16–N11	1.347	C5–N1–N2	115.1 (2)
N1–N2	1.378	C6–N2–N1	121.2 (2)
N4–N5	1.369	C13–N7–N8	116.3 (2)
N7–N8	1.371	C14–N8–N7	120.0 (2)
N10–N11	1.373	C15–N10–N11	115.5 (2)

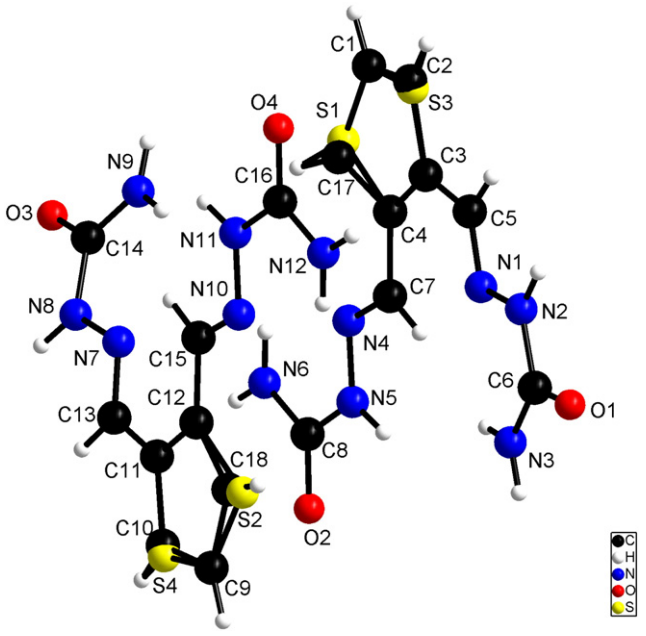

Fig. 4. Crystal structure and atoms numbering for 2,3BSTCH$_2$.

The crystal structure displays many hydrogen bonds (Table 5) between bis(semicarbazone), water molecule and bromide ions forming a three-dimensional network. The molecular packing diagram is show in Fig. 7, hydrogen bondings have been omitted for clarity (Fig. 7). These bonds appeared between a hydrogen atom from a NH group in a complex molecule and a bromide ion in a neighbour unit cell.

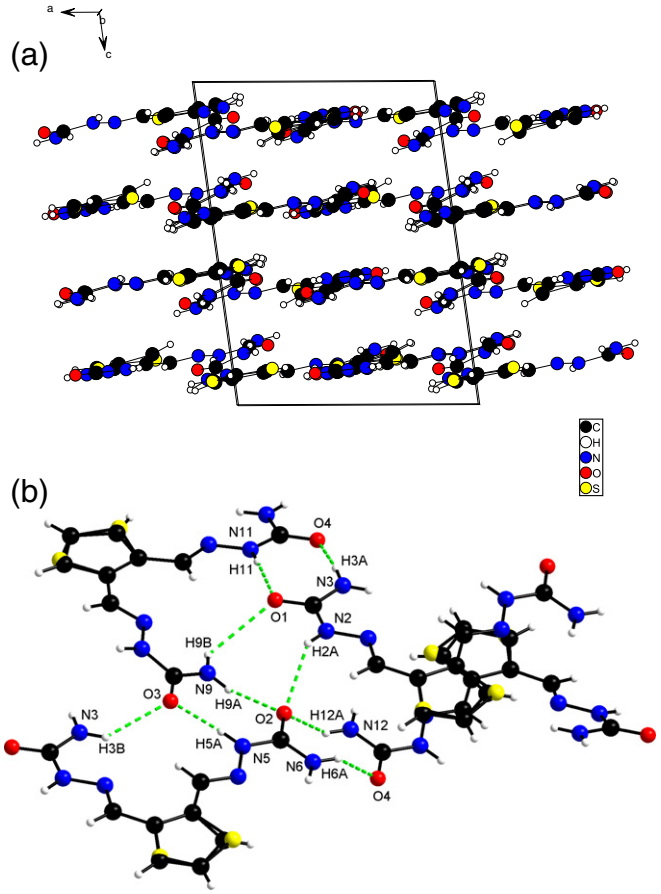

Fig. 5. Cell packing (a) and hydrogen bonding (b) for 2,3BSTCH$_2$.

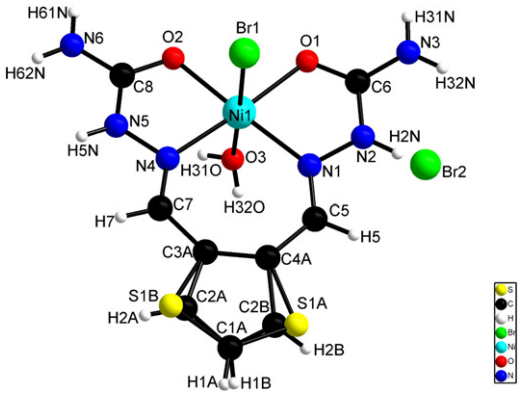

Fig. 6. Crystal structure and atoms numbering for [NiBr(2,3BSTCH$_2$)(H$_2$O)]Br.

This bromide ion is also linked, via a second hydrogen bond, to a water molecule.

3.3. Structures of complexes

3.3.1. Analytical data

The elemental analysis of the ligands and their complexes is summarised in Table 6. A good harmony between the experimental and calculated values is observed and the formulae of the complexes are: [NiCl$_2$(3STCH)$_2$], [NiBr$_2$(3STCH)$_2$], [NiCl(2,3BSTCH$_2$)(H$_2$O)]Cl and [NiBr(2,3BSTCH$_2$)(H$_2$O)]Br respectively.

The melting points were determined using Differential Scanning Calorimetry (DSC). In all complexes, the decomposition follows the beginning of the melting process.

3.3.2. Infrared spectra

The main infrared vibration bands are reported in Table 7. In principle, since the ligands contain a carbonyl functional group, it can exhibit the ketone–enol tautomerism. The ν(OH) band around 3350 cm^{-1} is absent from the IR spectra of the ligands but the ν(N–H) band at 3163 (3STCH) and 3146 cm^{-1} (2,3BSTCH$_2$) is present, indicating that, in the solid state, the ligands stand as the ketone tautomer. The spectrum of the ligands exhibits a strong band at 1685 cm^{-1}, due to the C═O stretching vibration [5].

In the case of the nickel complexes of 3STCH, [NiCl$_2$(3STCH)$_2$] and [NiBr$_2$(3STCH)$_2$], the ν(NH$_2$) vibration band is slightly shifted to lower wavenumbers whereas ν(N–H) is shifted to higher values (Table 7). The ring breathing remains quite unchanged when passing from ligands to complexes at ca. 832 cm^{-1}. In the mean time, the band corresponding to ν(C═N) is not significantly modified. The ν(C═O) vibration band is

Table 4
Bond lengths (Å) and angles (°) for the complex [NiBr(2,3BSTCH$_2$)(H$_2$O)]Br.

Bond lengths		Bond angles	
Ni1 – Br1	2.620	Br1 – Ni1 – O1	90.46
Ni1 – O1	2.022	Br1 – Ni1 – O2	92.10
Ni1 – O2	2.011	Br1 – Ni1 – O3	178.38
Ni1 – O3	2.143	Br1 – Ni1 – N1	92.64
Ni1 – N1	2.013	Br1 – Ni1 – N4	88.97
Ni1 – N4	2.018	O1 – Ni1 – O2	94.61
O1 – C6	1.244	O1 – Ni1 – O3	89.96
O2 – C8	1.253	O1 – Ni1 – N1	81.02
N1 – C5	1.277	O1 – Ni1 – N4	176.14
N1 – N2	1.381	O2 – Ni1 – O3	86.31
N2 – C6	1.366	O2 – Ni1 – N1	173.58
N3 – C6	1.316	O2 – Ni1 – N4	81.59
N4 – C7	1.282	O3 – Ni1 – N1	88.97
N4 – N5	1.376	O3 – Ni1 – N4	90.51
N5 – C8	1.359	N1 – Ni1 – N4	102.82
N6 – C8	1.328	Ni1 – N1 – N2	109.35

Table 5
Bond lengths (Å), angles (°) of intermolecular hydrogen bonds for ligands and Ni (II) complex.

Compound	D–H…A	*d*(H…A) (Å)	*d*(D…A) (Å)	Angle (°)
3STCH	N1–H1A…O1	1.94	2.89	169.30
	N2–H2A…O1	2.16	2.92	174.02
$2,3BSTCH_2$	N11–H11…O1	2.07	2.92	170.45
	N9–H9B…O1	2.78	3.28	118.98
	N2–H2A…O2	2.39	3.05	134.40
	N9–H9A…O2	2.16	2.98	157.40
	N12–H12A…O2	2.25	2.98	141.67
	N5–H5A…O3	1.99	2.85	176.09
	N3–H3B…O3	2.49	3.13	131.64
	N3–H3A…O4	2.05	2.89	166.11
	N6–H6A…O4	2.25	2.96	140.67
$[NiBr(2,3BSTCH_2)(H_2O)]Br$	N2–H2n…Br1	3.05	3.79	146.00
	N2–H2n…Br2	2.95	3.38	113.00
	N3–H31n…Br1	2.67	3.53	172.00
	N3–H32n…Br1	2.76	3.55	154.00
	N5–H5n…Br2	2.45	3.24	152.00
	N6–H61n…O2	2.37	3.06	138.00
	N6–H62n…O3	2.35	3.16	157.00
	N6–H61n…O1	2.62	3.21	128.00
	O3–H31o…Br1	2.66	3.35	153.00
	O3–H32…Br2o	2.47	3.20	168.00

Table 6
Analytical data.

Compound	Colour	Yield (%)	MP (°C)	Elemental analysis found (Calc.)		
				C (%)	H (%)	N (%)
3STCH	Yellow	90	231	42.37 (42.59)	3.96 (4.17)	24.57 (24.83)
$2,3BSTCH_2$	Yellow	88	224	36.83 (37.79)	4.06 (3.96)	32.82 (33.05)
$[NiCl_2(3STCH)_2]$	Green	67	213	29.78 (30.80)	3.22 (3.02)	17.23 (17.96)
$[NiBr_2(3STCH)_2]$	Green	60	231	26.72 (25.88)	2.35 (2.53)	15.21 (15.09)
$[NiCl(2,3BSTCH_2)(H_2O)]Cl$	Dark green	70	209	23.87 (23.91)	2.97 (3.01)	20.69 (20.91)
$[NiBr(2,3BSTCH_2)(H_2O)]Br$	Dark green	73	269	19.66 (19.58)	2.50 (2.46)	17.30 (17.12)

significantly shifted to lower wavenumbers. In addition, the spectra of these nickel complexes show the three vibration bands ν(M–O), ν(M–N) and ν (M–X) at 350, 527 and 227 cm^{-1} respectively, indicating that the coordinating atoms are O atom (keto) and N atom (imino) for each ligand.

In the spectra of the complexes of $2,3BSTCH_2$, $[NiCl(2,3BSTCH_2)(H_2O)]Cl$ and $[NiBr(2,3BSTCH_2)(H_2O)]Br$, we find the same shifts for $\nu(NH_2)$, ν(N–H) and ν(C═O) bands than in the case of the nickel complex of 3STCH. In addition, the band ν(OH) is located at 3355 and 3358 cm^{-1} for these two compounds. These results show that the coordination and the structures of the choro of the bromo complexes are very similar.

3.3.3. Structures of the complexes

The proposed structures of the complexes $[NiCl_2(3STCH)_2]$, $[NiBr_2(3STCH)_2]$ are given in Fig. 8. They were determined from their spectroscopic data and their DSC diagrams revealing a similar behaviour for the two complexes. In these compounds, the coordinating atoms are O (keto) and N (imino) for each ligand. In an octahedral geometry, the nickel (II) ion is linked to the two ligands with the O and N atoms in the same plane, while the two halogenides are located on the orthogonal axis to this plane. This structure was already observed for similar compounds with semicarbazone functional group [5].

The structure of $[NiCl(2,3BSTCH_2)(H_2O)]Cl$ was determined on the basis of the crystal structure of the $[NiBr(2,3BSTCH_2)(H_2O)]Br$. As their spectroscopic data are similar, the chloro compound is identical to the bromo one (Fig. 8).

3.4. Biological activities

Antifungal assays (Table 8) showed that both, 3STCH and $2,3BSTCH_2$ are inactive against all strains, although the corresponding complexes exhibited a moderate activity (31 to 5 $\mu g.mL^{-1}$) specifically on *C. glabrata*. In Fig. 9, the shortest bars corresponding to higher activity are observed for $[NiCl_2(3STCH)_2]$ (*2*), $[NiBr_2(3STCH)_2]$ (*3*), $[NiCl(2,3BSTCH_2)(H_2O)]Cl$ (*5*) and $[NiBr(2,3BSTCH_2)(H_2O)]Br$ (*6*) against *C. glabrata*. As the MIC_{80} values for Amphotericin are very low, they are not visible on this chart.

The determined MIC_{80} values revealed that complexes deriving from $2,3BSTCH_2$ are slightly more active than the corresponding 3STCH ones. Basis on molar concentrations, $[NiBr(2,3BSTCH_2)(H_2O)]Br$ is 3.5 times more active (31 $\mu g.mL^{-1}$ or 6.31×10^{-5} M) than $[NiBr_2(3STCH)_2]$ (125 $\mu g.mL^{-1}$ or 2.25×10^{-4} M). On the opposite side, the chloro-complexes exhibit some similar activity the MIC_{80} is 62 $\mu g.mL^{-1}$

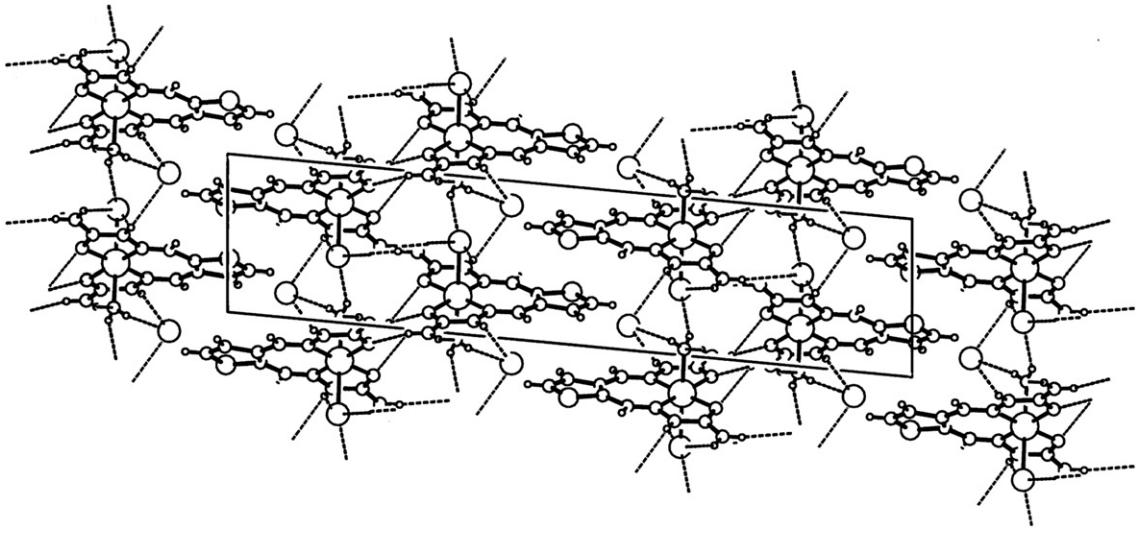

Fig. 7. Cell packing and hydrogen bonding for $[NiBr(2,3BSTCH_2)(H_2O)]Br$.

Table 7
Infrared data for the ligands and the complexes (cm^{-1}).

Compound	$\nu(NH_2)$	$\nu(OH)$	$\nu(NH)$	$\nu(C{=}N)$	$\nu(C{=}O)$	Resp. cycle	$\nu(N-N)$	$\nu(M-N)$	$\nu(M-O)$	$\nu(M-X)$
3STCH	3450	–	3163	1648	1685	820	942	–	–	–
$2,3BSTCH_2$	3464	–	3109	1594	1684	758	931	–	–	–
$[NiCl_2(3STCH)_2]$	3449	–	3291	1639	1673	832	942	527	350	227
$[NiBr_2(3STCH)_2]$	3434	–	3168	1605	1668	832	942	532	348	224
$[NiCl(2,3BSTCH_2)(H_2O)]Cl$	3480	3355	3151	1600	1674	777	952	440	335	227
$[NiBr(2,3BSTCH_2)(H_2O)]Br$	3482	3358	3147	1601	1670	811	930	503	322	223

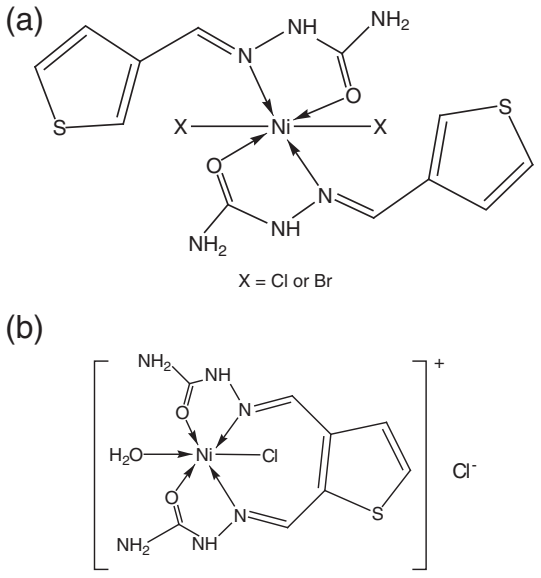

Fig. 8. Structures of the complexes $[NiCl_2(3STCH)_2]$, $[NiBr_2(3STCH)_2]$ (a) and $[NiCl(2,3BSTCH_2)(H_2O)]Cl$ (b).

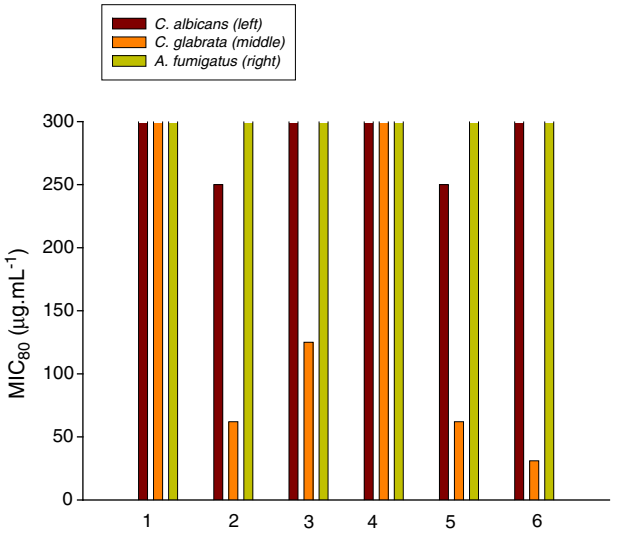

Fig. 9. Compared MIC_{80} for the ligands 1 and 4 and the complexes 2–3 and 5–6 (numbers refer to Table 8).

$(1.54\times10^{-4}$ M) for $[NiCl(2,3BSTCH_2)(H_2O)]Cl$ and 62 µg.mL^{-1} $(1.32\times10^{-4}$ M) for $[NiCl_2(3STCH)_2]$.

A weak or no activity was found for all the compounds at 10^{-5} M against MRC5 cells lines, suggesting the absence of cytotoxicity as well as their potential interest on human pathogenic yeasts. These results differ from those previously described in our laboratory with 2-furfural semicarbazone and 5-methyl 2-furfural semicarbazone for which the copper (II) complexes exhibited a cytotoxic activity [36,37]. So these new complexes with thiophen semicarbazones could be eventually used against *C. glabrata* after testing a large number of strains to confirm this activity.

In addition, no activity was found for all the compounds on solid media (data not shown). Nevertheless, as it was already reported [38], these results could indicate that increasing steric hindrance and molar molecular weight lead to restricted diffusion on solid media because of their increasing lipophilic character as previously reported for manganese complexes [15]. It is also asses the importance of antifungal testing on liquid medium.

4. Conclusion

We have synthesised and characterised two new ligands bearing respectively one and two semicarbazone moieties: 3STCH and $2,3BSTCH_2$. These molecules lead to four new complexes with Ni (II). The complexes obtained with 3STCH are similar to those described with various monosemicarbazones. The bis(semicarbazone) $2,3BSTCH_2$ allows us to obtain the complexes $[NiX(2,3BSTCH_2)(H_2O)]X$ (X = Cl or Br) which have not been described for semicarbazones nickel complexes. Finally the determination of MIC_{80} values against *C. albicans*, *C. glabrata* and *A. fumigatus* revealed that the ligands are quite inactive against all strains, while complexes deriving from $2,3BSTCH_2$ are more active than the corresponding 3STCH ones against *C. glabrata*.

Table 8
Antifungal activity of the ligands and the complexes (minimal concentration inhibiting 80% of fungal growth or MIC_{80}) expressed in µg.mL^{-1}.

Compound (*number*)	Fungi		
	Candida albicans ATTC 66396	*Candida glabrata* LMA 1085	*Aspergillus fumigatus* CBS 11326
3STCH (*1*)	>250	>250	>250
$[NiCl_2(3STCH)_2]$ (*2*)	250	62	>250
$[NiBr_2(3STCH)_2]$ (*3*)	>250	125	>250
$2,3BSTCH_2$ (*4*)	>250	>250	>250
$[NiCl(2,3BSTCH_2)(H_2O)]Cl$ (*5*)	250	62	>250
$[NiBr(2,3BSTCH_2)(H_2O)]Br$ (*6*)	>250	31	>250
Amphotericine B	0.062	0.125	6

Appendix A. Supplementary data

CCDC 855944 (3STCH), 855943 (2,3BSTCH$_2$) and 855897 ([NiBr(2,3BSTCH$_2$)(H$_2$O)]Br) contain the supplementary crystallographic data for this paper. These data can be obtained free of charge from the Cambridge Crystallographic Data Centre CCDC (12 Union Road. Cambridge, CB2 IEZ, UK; fax: +44 1223 336033; e-mail: deposit@ccdc.cam.ac.uk) or via www.ccdc.cam.ac.uk/data_request/cif. Supplementary data to this article can be found online at http://dx.doi.org/10.1016/j.jinorgbio.2012.04.022.

References

[1] J.S. Casas, M.S. García-Tasende, J. Sordo, Coord. Chem. Rev. 209 (2000) 197–261.
[2] H. Beraldo, D. Gambino, Mini-Rev. Med. Chem. 4 (2004) 31–39.
[3] Z. Afrasiabi, E. Sinn, W. Lin, Y. Ma, C. Campana, S. Padhye, J. Inorg. Biochem. 99 (2005) 1526–1531.
[4] M.C. Rodriguez-Argüelles, S. Mosquera-Vàzquez, J. Sanmartin-Matalobos, A.M. Garcia-Deibe, C. Pelizzi, F. Zani, Polyhedron 29 (2010) 864–870.
[5] S. Chandra, L.K. Gupta, Spectrochim. Acta A 62 (2005) 1089–1094.
[6] V.L. Siji, M.R. Sudarsanakumar, S. Suma, Polyhedron 29 (2010) 2035–2040.
[7] A. Pérez-Rebolledo, O.E. Piro, E.E. Castellano, L.R. Teixeira, A.A. Batista, H. Beraldo, J. Mol. Struct. 794 (2006) 18–23.
[8] L. Otero, P. Noblia, D. Gambino, H. Cerecetto, M. Gonzàlez, J.A. Elena, O.E. Piro, Inorg. Chim. Acta 344 (2003) 85–94.
[9] T.A. Reena, E.B. Seena, M.R. Prathapachandra Kurup, Polyhedron 27 (2008) 1825–1831.
[10] G. Ibrahim, M.A. Khan, P. Richomme, O. Benali-Baïtich, G. Bouet, Polyhedron 16 (1997) 3455–3461.
[11] G. Ibrahim, E. Chebli, M.A. Khan, G.M. Bouet, Transition Met. Chem. 24 (1999) 294–298.
[12] J.E. Karp, F.J. Giles, I. Gojo, L. Morris, J. Greer, B. Johnson, M. Thein, M. Sznol, J. Low, Leuk. Res. 32 (2008) 71–77.
[13] R. Ramachandran, M. Rani, S. Kabilan, Bioorg. Med. Chem. Lett. 19 (2009) 2819–2823.
[14] C. Costello, T. Karpanen, P.A. Lambert, P. Mistry, K.J. Parker, D.L. Rathbone, J. Ren, L. Wheeldon, T. Worthington, Bioorg. Med. Chem. Lett. 18 (2008) 1708–1711.
[15] S. Belaïd, A. Landreau, S. Djebbar, O. Benali-Baïtich, G. Bouet, J.P. Bouchara, J. Inorg. Biochem. 102 (2008) 63–69.
[16] G.L. Parrilha, J.G. Da Silva, L.F. Gouveia, A.K. Gasparoto, R.P. Dias, W.R. Rocha, D.A. Santos, N.L. Speziali, H. Beraldo, Eur. J. Med. Chem. 46 (2011) 1473–1482.
[17] I.C. Mendes, M.A. Soares, R.G. Dos Santos, C. Pinheiro, H. Beraldo, Eur. J. Med. Chem. 44 (2009) 1870–1877.
[18] J.G. Da Silva, L.S. Azzolini, S.M.S.V. Wardell, J.L. Wardell, H. Beraldo, Polyhedron 28 (2009) 2301–2305.
[19] K. Alomar, A. Landreau, M. Kempf, M.A. Khan, M. Allain, G. Bouet, J. Inorg. Biochem. 104 (2010) 397–404.
[20] K. Alomar, M.A. Khan, M. Allain, G. Bouet, Polyhedron 28 (2009) 1273–1281.
[21] G.M. Sheldrick, SHELX97 — Program for Crystal Structure Analysis (Release 97–2), , 1998.
[22] Bruker-Axs, APEX2, Bruker Analytical X-ray Systems Inc., Madison, Wisconsin, USA, 2009.
[23] Bruker-Axs, SAINT and SADABS, Bruker Analytical X-ray Systems Inc., Madison, Wisconsin, USA, 2009.
[24] G.M. Sheldrick, SHELXS97 and SHELXL97, Universität Göttingen, Göttingen, Germany, 1997.
[25] E. Lukevics, L. Ignatovich, S. Belyakov, Chem. Heterocycl. Compd. 43 (2007) 243–249.
[26] National Committee for Clinical Laboratory Standards, Reference Method for Broth Dilution Antifungal Susceptibility Testing of Yeasts, Approved standard M27-A., Villanova, PA, 1997.
[27] National Committee for Clinical Laboratory Standards, Reference Method for Broth Dilution Antifungal Susceptibility Testing of Filamentous Fungi, Approved Standard, NCCLS Document M38-A, , Clinical and Laboratory Standards Institute, Villanova, PA, 2002.
[28] V. Moret, Y. Laras, T. Cresteil, G. Aubert, D.Q. Ping, C. Di, M. Barthélémy-Requin, V.P.C. Béclin, D. Allegro, A. Rolland, F. De Angelis, E. Gatti, P. Pierre, L. Pasquini, E. Petrucci, U. Testa, J.-L. Kraus, Eur. J. Med. Chem. 44 (2009) 558–567.
[29] A. Sreekanth, U.L. Kala, C.R. Nayar, M.R. Prathapachandra Kurup, Polyhedron 23 (2004) 41–47.
[30] E. López-Torres, M.A. Mendiola, C.J. Pastor, Polyhedron 28 (2009) 221–226.
[31] A. Trzesowska, J. Mol. Struct. 917 (2009) 125–132.
[32] H. Beraldo, R. Lima, L.R. Teixeira, A.A. Moura, D.X. West, J. Mol. Struct. 559 (2001) 99–106.
[33] G.J. Palenik, D.W. Wester, U. Rychlewska, R.C. Palenik, Inorg. Chem. 15 (1976) 1814–1819.
[34] K.B. Gudasi, S.A. Patil, R.S. Vadavi, R.V. Shenoy, N. Nethaji, S.W.A. Bligh, Inorg. Chim. Acta 359 (2006) 322–3236.
[35] G.J. Palenik, D.W. Wester, Inorg. Chem. 17 (1978) 864–870.
[36] (WOS:000165934700012). I.H. Hall, C.B. Lackey, T.D. Kistler, R.W. Durham, E.M. Jouad, M. Khan, X.D. Thanh, S. Djebbar-Sid, O. Benali-Baitich, G.M. Bouet, Pharmazie 55 (2000) 937–941.
[37] I. Hall, C. Lee, G. Ibrahim, M.A. Khan, G. Bouet, Appl. Organomet. Chem. 11 (1997) 565–575.
[38] S. Shreaz, R.A. Sheikh, R. Bhatia, K. Neelofar, S. Imran, A.A. Hashmi, N. Manzoor, S.F. Basir, L.A. Khan, Biometals 24 (2011) 923–933.